

A METHOD FOR SEPARATING THE PHYSICS FROM THE ASTROPHYSICS OF HIGH-REDSHIFT 21CM FLUCTUATIONS

RENNAN BARKANA¹ & ABRAHAM LOEB²

Draft version September 29, 2018

ABSTRACT

Fluctuations in the 21cm brightness from cosmic hydrogen at redshifts $z \gtrsim 6$ were sourced by the primordial density perturbations from inflation as well as by the radiation from galaxies. We propose a method to separate these components based on the angular dependence of the 21cm fluctuation power spectrum. Peculiar velocities increase the power spectrum by a factor of ~ 2 compared to density fluctuations alone, and introduce an angular dependence in Fourier space. The resulting angular structure relative to the line of sight facilitates a simple separation of the power spectrum into several components, permitting an unambiguous determination of the primordial power spectrum of density fluctuations, and of the detailed properties of all astrophysical sources of 21cm fluctuations. We also demonstrate that there is no significant information to be gained from 21cm measurements on large angular scales. Thus, observational analyses can be confined to small angular areas where projection effects are negligible, and theoretical predictions should focus on the three-dimensional power spectrum of 21cm fluctuations.

Subject headings: galaxies: high-redshift, cosmology: theory, galaxies: formation

1. INTRODUCTION

Following the recombination of protons and electrons less than a million years after the big bang, the universe was filled with neutral hydrogen (H I). Hundreds of millions of years later, the first galaxies began to reionize the cosmic gas (Barkana & Loeb 2001). The spectra of the farthest quasars indicate that reionization completed at a redshift $z \sim 6$, a billion years after the big bang (Fan et al. 2002; White et al. 2003; Wyithe et al. 2004). The hyperfine spin-flip transition of H I at a wavelength of 21 cm provides the most promising tracer of the cosmic gas before the end of reionization. Several groups are currently constructing low-frequency radio arrays capable of detecting the diffuse 21cm radiation (<http://space.mit.edu/eor-workshop/>). Since this radiation interacts with H I through a resonant transition, any observed wavelength selects a redshift slice of the universe. Future measurements of the redshifted 21cm brightness as a function of wavelength and direction should provide a three-dimensional map of the cosmic H I (Hogan & Rees 1979; Madau et al. 1997). Fluctuations in the 21cm brightness are sourced by primordial density inhomogeneities on all scales down to the cosmological Jeans mass, making 21cm the richest cosmological data set on the sky (Loeb & Zaldarriaga 2004).

The 21cm signal can be seen from epochs during which the gas was largely neutral and deviated from thermal equilibrium with the cosmic microwave background (CMB). The signal vanished at redshifts $z \gtrsim 200$, when the residual fraction of free electrons after cosmological recombination kept the gas kinetic temperature, T_k , close to the CMB temperature, T_γ . But during $200 \gtrsim z \gtrsim 30$ the gas cooled adiabatically and atomic collisions kept the spin temperature of the hyperfine level population below T_γ , so that the gas appeared in absorption (Scott & Rees 1990; Loeb & Zaldarriaga 2004).

As the Hubble expansion continued to rarefy the gas, radiative coupling of T_s to T_γ began to dominate and the 21cm signal faded. When the first galaxies formed, the UV photons they produced between the Ly α and Lyman limit wavelengths propagated freely through the universe, redshifted into the Ly α resonance, and coupled T_s and T_k once again through the Wouthuysen-Field (Wouthuysen 1952; Field 1958) effect by which the two hyperfine states are mixed through the absorption and re-emission of a Ly α photon (Madau et al. 1997; Ciardi & Madau 2003). Emission of UV photons above the Lyman limit by the same galaxies initiated the process of reionization by creating ionized bubbles in the neutral cosmic gas, while X-ray photons propagated farther and heated T_k above T_γ throughout the universe. Once T_s grew larger than T_γ , the gas appeared in 21cm emission. The ionized bubbles imprinted a knee in the power spectrum of 21cm fluctuations (Zaldarriaga et al. 2004), which traced the H I topology until the process of reionization was completed (Furlanetto et al. 2004a).

The various effects that determine the 21cm fluctuations can be separated into two classes. On the one hand, the density power spectrum probes basic cosmological parameters and inflationary initial conditions, and can be calculated exactly in linear theory. On the other hand, the radiation from galaxies, both Ly α radiation and ionizing photons, involves the complex, non-linear physics of galaxy formation and star formation. If only the sum of all fluctuations could be measured, then it would be difficult to extract the separate sources, and in particular, the extraction of the power spectrum would be subject to systematic errors involving the properties of galaxies. We show in this *Letter* that the unique three-dimensional properties of 21cm measurements permit a separation of these distinct effects. Thus, 21cm fluctuations can probe astrophysical (radiative) sources during the epoch of first galaxies, while at the same time separately probing physical (inflationary) sources. In order to affect this separation most easily, it is necessary to measure the three-dimensional power spectrum of 21cm fluctuations, while full-sky observations are normally restricted to angular projections. However, we show that unlike the analogous case of CMB fluctuations,

¹ School of Physics and Astronomy, The Raymond and Beverly Sackler Faculty of Exact Sciences, Tel Aviv University, Tel Aviv 69978, ISRAEL; barkana@wise.tau.ac.il

² Astronomy Department, Harvard University, 60 Garden Street, Cambridge, MA 02138; aloeb@cfa.harvard.edu

21cm measurements on large angular scales are not useful. Thus, observational analyses can be confined to small angular areas where projection effects are negligible.

2. SPIN TEMPERATURE HISTORY

The spin temperature T_s is defined through the ratio between the number densities of hydrogen atoms in the excited and ground state levels, $n_1/n_0 = (g_1/g_0)\exp\{-T_\star/T_s\}$, where subscripts 1 and 0 correspond to the excited and ground state levels of the 21cm transition, $(g_1/g_0) = 3$ is the ratio of the spin degeneracy factors of the levels, and $T_\star = 0.0682\text{K}$ corresponds to the energy difference between the levels. As long as T_s is smaller than the CMB temperature $T_\gamma = 2.725(1+z)\text{K}$, hydrogen atoms absorb the CMB, whereas if $T_s > T_\gamma$ they emit excess flux. In general, the resonant 21cm interaction changes the brightness temperature of the CMB by (Scott & Rees 1990; Madau et al. 1997) $T_b = \tau(T_s - T_\gamma)/(1+z)$, where the optical depth at a wavelength $\lambda = 21\text{cm}$ is

$$\tau = \frac{3c\lambda^2 h A_{10} n_H}{32\pi k_B T_s (1+z) (dv_r/dr)} x_{\text{HI}}, \quad (1)$$

where n_H is the number density of hydrogen, $A_{10} = 2.85 \times 10^{-15} \text{ s}^{-1}$ is the spontaneous emission coefficient, x_{HI} is the neutral hydrogen fraction, and dv_r/dr is the gradient of the radial velocity along the line of sight with v_r being the physical radial velocity and r the comoving distance; on average $dv_r/dr = H(z)/(1+z)$ where H is the Hubble parameter. The velocity gradient term arises since the 21cm scattering cross-section has a fixed thermal width which translates through the redshift factor $(1+v_r/c)$ to a fixed interval in velocity (Sobolev 1960).

For the concordance set of cosmological parameters (Spergel et al. 2003), the mean brightness temperature on the sky at redshift z is $T_b = 28\text{mK}[(1+z)/10]^{1/2}[(T_s - T_\gamma)/T_s]\bar{x}_{\text{HI}}$, where \bar{x}_{HI} is the mean neutral fraction of hydrogen. The spin temperature itself is coupled to T_k through the spin-flip transition, which can be excited by collisions or by the absorption of Ly α photons. As a result, the combination that appears in T_b becomes (Field 1958) $(T_s - T_\gamma)/T_s = [x_{\text{tot}}/(1+x_{\text{tot}})](1 - T_\gamma/T_k)$, where $x_{\text{tot}} = x_\alpha + x_c$ is the sum of the radiative and collisional threshold parameters. These parameters are $x_\alpha = 4P_\alpha T_\star/27A_{10}T_\gamma$ and $x_c = 4\kappa_{1-0}(T_k)n_H T_\star/3A_{10}T_\gamma$, where P_α is the Ly α scattering rate which is proportional to the Ly α intensity, and κ_{1-0} is tabulated as a function of T_k (Allison & Dalgarno 1969; Zygelman 2004). The coupling of the spin temperature to the gas temperature becomes substantial when $x_{\text{tot}} \gtrsim 1$.

3. BRIGHTNESS TEMPERATURE FLUCTUATIONS

Although the mean 21cm emission or absorption is difficult to measure due to bright foregrounds, the unique character of the fluctuations in T_b allows for a much easier extraction of the signal (Gnedin & Shaver 2003; Zaldarriaga et al. 2004; Morales & Hewitt 2004; Morales 2004; Santos et al. 2004). In general, the fluctuations in T_b can be sourced by fluctuations in gas density, temperature, neutral fraction, radial velocity gradient, and Ly α flux (through x_α). Adopting the notation δ_A for the fractional fluctuation in quantity A (with a lone δ denoting density perturbations), we find

$$\delta_{T_b} = \left(1 + \frac{x_c}{\tilde{x}_{\text{tot}}}\right)\delta + \frac{x_\alpha}{\tilde{x}_{\text{tot}}}\delta_{x_\alpha} + \delta_{x_{\text{HI}}} - \delta_{d_r v_r} + (\gamma_a - 1) \left[\frac{T_\gamma}{T_k - T_\gamma} + \frac{x_c}{\tilde{x}_{\text{tot}}} \frac{d \log(\kappa_{1-0})}{d \log(T_k)} \right] \delta, \quad (2)$$

where the adiabatic index is $\gamma_a = 1 + (\delta_{T_k}/\delta)$, and we define $\tilde{x}_{\text{tot}} \equiv (1+x_{\text{tot}})x_{\text{tot}}$. Taking the Fourier transform, we obtain the power spectrum of each quantity; e.g., the total power spectrum P_{T_b} is defined by

$$\langle \tilde{\delta}_{T_b}(\mathbf{k}_1) \tilde{\delta}_{T_b}(\mathbf{k}_2) \rangle = (2\pi)^3 \delta^D(\mathbf{k}_1 + \mathbf{k}_2) P_{T_b}(\mathbf{k}_1), \quad (3)$$

where $\tilde{\delta}_{T_b}(\mathbf{k})$ is the Fourier transform of δ_{T_b} , \mathbf{k} is the comoving wavevector, and $\langle \dots \rangle$ denotes an ensemble average.

4. THE SEPARATION OF POWERS

The fluctuation δ_{T_b} consists of a number of isotropic sources of fluctuations plus the peculiar velocity term $-\delta_{d_r v_r}$. Its Fourier transform is simply proportional to that of the density field (Kaiser 1987; Bharadwaj & Ali 2004a),

$$\tilde{\delta}_{d_r v_r} = -\mu^2 \tilde{\delta}, \quad (4)$$

where $\mu = \cos \theta_k$ in terms of the angle θ_k of \mathbf{k} with respect to the line of sight. The μ^2 dependence in this equation results from taking the radial component ($\propto \mu$) of the peculiar velocity, and then the radial component ($\propto \mu$) of its gradient. Intuitively, a high-density region possesses a velocity infall towards the density peak, implying that a photon must travel further from the peak in order to reach a fixed relative redshift, compared with the case of pure Hubble expansion. Thus the optical depth is always increased by this effect in regions with $\delta > 0$. This phenomenon is most properly termed *velocity compression*.

We therefore write the fluctuation in Fourier space as

$$\tilde{\delta}_{T_b}(\mathbf{k}) = \mu^2 \tilde{\delta}(\mathbf{k}) + \beta \tilde{\delta}(\mathbf{k}) + \tilde{\delta}_{\text{rad}}(\mathbf{k}), \quad (5)$$

where we have defined a coefficient β by collecting all terms $\propto \delta$ in equation (2), and have also combined the terms that depend on the radiation fields of Ly α photons and ionizing photons, respectively. We assume that these radiation fields produce isotropic power spectra, since the physical processes that determine them have no preferred direction in space. The total power spectrum is

$$P_{T_b}(\mathbf{k}) = \mu^4 P_\delta(k) + 2\mu^2 [\beta P_\delta(k) + P_{\delta-\text{rad}}(k)] + [\beta^2 P_\delta(k) + P_{\text{rad}}(k) + 2\beta P_{\delta-\text{rad}}(k)], \quad (6)$$

where we have defined the power spectrum $P_{\delta-\text{rad}}$ as the Fourier transform of the cross-correlation function,

$$\xi_{\delta-\text{rad}}(r) = \langle \delta(\mathbf{r}_1) \delta_{\text{rad}}(\mathbf{r}_1 + \mathbf{r}) \rangle. \quad (7)$$

We note that a similar anisotropy in the power spectrum has been previously derived in a different context, that of measuring density fluctuations from galaxy redshift surveys. In that case, the use of redshifts to estimate distances changes the apparent density of galaxies along the line of sight (Kaiser 1987; Lilje & Efstathiou 1989; Hamilton 1992; Fisher, Scharf, & Lahav 1994). However, in the case of galaxies there is no analog to the method that we demonstrate below for separating in 21cm fluctuations the effect of initial conditions from that of later astrophysical processes.

We may now calculate the angular power spectrum of the brightness temperature on the sky at a given redshift – corresponding to a comoving distance r_0 along the line of sight. The brightness fluctuations can be expanded in spherical harmonics with expansion coefficients $a_{lm}(\nu)$, where the angular power spectrum

$$C_l(r_0) = \langle |a_{lm}(\nu)|^2 \rangle = 4\pi \int \frac{d^3 k}{(2\pi)^3} \left[G_l^2(kr_0) P_\delta(k) + 2P_{\delta-\text{rad}}(k) G_l(kr_0) j_l(kr_0) + P_{\text{rad}}(k) j_l^2(kr_0) \right], \quad (8)$$

with $G_l(x) \equiv J_l(x) + (\beta - 1)j_l(x)$ and $J_l(x)$ being a linear combination of spherical Bessel functions (Bharadwaj & Ali 2004a).

The velocity gradient term has been previously neglected in 21cm calculations, except for its effect on the sky-averaged power and on radio visibilities (Tozzi et al. 2000; Bharadwaj & Ali 2004a,b). In the simple case where $\beta = 1$ and only the density and velocity terms contribute, the velocity term increases the total power by a factor of $\langle (1 + \mu^2)^2 \rangle = 1.87$ in the spherical average. However, instead of averaging the signal, we can use the angular structure of the power spectrum to greatly increase the discriminatory power of 21cm observations. We may break up each spherical shell in \mathbf{k} space into rings of constant μ and construct the observed $P_{T_b}(k, \mu)$. Considering equation (6) as a polynomial in μ , i.e., $\mu^4 P_{\mu^4} + \mu^2 P_{\mu^2} + P_{\mu^0}$, we see that the power at just three values of μ is required in order to separate out the coefficients of 1, μ^2 , and μ^4 for each k .

If the velocity compression were not present, then only the μ -independent term (times T_b^2) would be observed, and its separation into the five components (T_b , β , and three power spectra) would be difficult and subject to degeneracies. Once the power has been separated into three parts, however, the μ^4 coefficient can be used to measure the density power spectrum directly, with no interference from any other source of fluctuations. Since the overall amplitude of the power spectrum, and its scaling with redshift, are well determined from the combination of the CMB temperature fluctuations and galaxy surveys, the amplitude of P_{μ^4} directly determines the mean brightness temperature T_b on the sky, which measures a combination of T_s and \bar{x}_{HI} at the observed redshift. Once $P_\delta(k)$ has been determined, the coefficients of the μ^2 term and the μ -independent term must be used to determine the remaining unknowns, β , $P_{\delta-\text{rad}}(k)$, and $P_{\text{rad}}(k)$. Since the coefficient β is independent of k , determining it and thus breaking the last remaining degeneracy requires only a weak additional assumption on the behavior of the power spectra, such as their asymptotic behavior at large or small scales. If the measurements cover N_k values of wavenumber k , then one wishes to determine $2N_k + 1$ quantities based on $2N_k$ measurements, which should not cause significant degeneracies when $N_k \gg 1$. Even without knowing β , one can probe whether some sources of $P_{\text{rad}}(k)$ are uncorrelated with δ ; the quantity $P_{\text{un}-\delta}(k) \equiv P_{\mu^0} - P_{\mu^2}^2 / (4P_{\mu^4})$ equals $P_{\text{rad}} - P_{\delta-\text{rad}}^2 / P_\delta$, which receives no contribution from any source that is a linear functional of the density distribution.

5. SPECIFIC EPOCHS

At $z \sim 35$, galaxy formation is in its infancy, while collisions are effective due to the high gas density (Loeb & Zaldarriaga 2004). Thus, $x_{\text{tot}} = x_c \gg x_\alpha$, $x_{\text{HI}} = 1$, and the gas cools adiabatically (with $\gamma_a = 5/3$). In addition to measuring the density power spectrum (Loeb & Zaldarriaga 2004), one can also trace the redshift evolution of n_{HI} , T_γ , and T_k , and verify that collisions are causing the fluctuations.

At $z \lesssim 35$, collisions become ineffective but the first stars produce a cosmic background of Ly α photons that couples T_s to T_k . During the period of initial Ly α coupling, fluctuations in the Ly α flux translate into fluctuations in the 21cm brightness (Barkana & Loeb 2004). This signal can be observed from $z \sim 25$ until the Ly α coupling is completed (i.e., $x_{\text{tot}} \gg 1$) at $z \sim 15$. At a given redshift, each atom sees Ly α photons that were originally emitted at earlier times at rest-frame wavelengths between Ly α and the Lyman limit. Distant sources

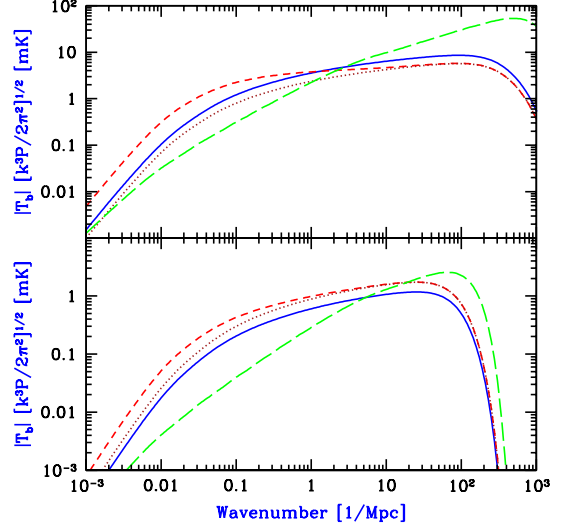


FIG. 1.— Observable power spectra during the period of initial Ly α coupling. *Upper panel*: Assumes adiabatic cooling. *Lower panel*: Assumes pre-heating to 500 K by X-ray sources. We show $P_{\mu^4} = P_\delta$ (solid curves), P_{μ^2} (short-dashed curves), and $P_{\text{un}-\delta}$ (long-dashed curves). We also show for comparison $2\beta P_\delta$ (dotted curves).

are time retarded, and since there are fewer galaxies in the distant, earlier universe, each atom sees sources only out to an apparent source horizon of ~ 100 comoving Mpc at $z \sim 20$. A significant portion of the flux comes from nearby sources, because of the $1/r^2$ decline of flux with distance, and since higher Lyman series photons, which are degraded to Ly α photons through scattering, can only be seen from a small redshift interval that corresponds to the wavelength interval between two consecutive atomic levels.

There are two separate sources of fluctuations in the Ly α flux (Barkana & Loeb 2004). The first is density inhomogeneities. Since gravitational instability proceeds faster in overdense regions, the biased distribution of rare galactic halos fluctuates much more than the global dark matter density. When the number of sources seen by each atom is relatively small, Poisson fluctuations provide a second source of fluctuations. Unlike typical Poisson noise, these fluctuations are correlated between gas elements at different places, since two nearby elements see many of the same sources. Assuming a scale-invariant spectrum of primordial density fluctuations, and that $x_\alpha = 1$ is produced at $z = 20$ by galaxies in dark matter halos where the gas cools efficiently via atomic cooling, we show in Figure 1 the predicted observable power spectra. The figure shows that β can be measured from the ratio P_{μ^2}/P_{μ^4} at $k \gtrsim 1 \text{ Mpc}^{-1}$, allowing the density-induced fluctuations in flux to be extracted from P_{μ^2} , while only the Poisson fluctuations contribute to $P_{\text{un}-\delta}$. Each of these components probes the number density of galaxies through its magnitude, and the distribution of source distances through its shape. Measurements at $k \gtrsim 100 \text{ Mpc}^{-1}$ can independently probe T_k because of the smoothing effects of the gas pressure and the thermal width of the 21cm line.

After Ly α coupling and X-ray heating are both completed, reionization continues. Since $\beta = 1$ and $T_k \gg T_\gamma$, the normalization of P_{μ^4} directly measures the mean neutral hydrogen fraction, and one can separately probe the density fluctuations, the neutral hydrogen fluctuations, and their cross-

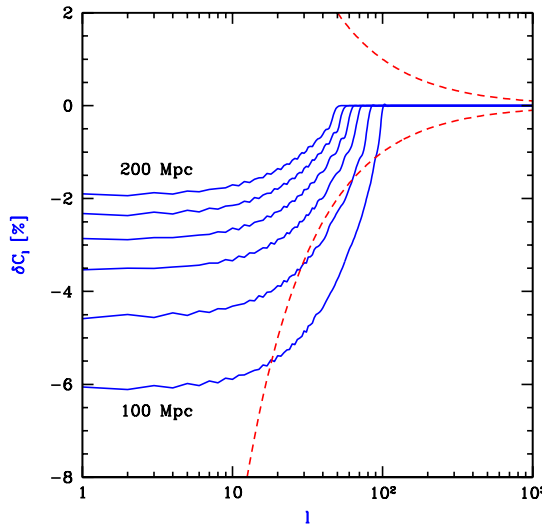


FIG. 2.— Effect of large-scale power on the angular power spectrum of 21cm anisotropies on the sky. This example shows the power from density fluctuations and velocity compression, assuming a hot IGM at $z = 12$ with $T_s = T_k \gg T_\gamma$. We show the % change in C_l if we were to cut off the power spectrum above $1/k$ of 200, 180, 160, 140, 120, and 100 Mpc (top to bottom). Also shown for comparison is the cosmic variance for averaging in bands of $\Delta l \sim l$ (dashed lines).

correlation.

6. FLUCTUATIONS ON LARGE ANGULAR SCALES

Full-sky observations must normally be analyzed with an angular and radial transform, rather than a Fourier transform which is simpler and yields more directly the underlying 3D power spectrum. In an angular transform on the sky, an angle of θ radians translates to a spherical multipole $l \sim 3.5/\theta$. For measurements on a screen at a comoving distance r_0 , a multipole l normally measures 3D power on a scale of $k^{-1} \sim \theta r_0 \sim 35/l$ Gpc for $l \gg 1$, since $r_0 \sim 10$ Gpc at $z \gtrsim 10$. This estimate fails at $l \lesssim 100$, however, when we consider the sources of 21cm fluctuations. The angular projection implied

in C_l involves a weighted average [equation (8)] which favors large scales when l is small, but density fluctuations possess little large-scale power, and the C_l are dominated by power around the peak of $kP_\delta(k)$, at a few tens of comoving Mpc.

Figure 2 shows that for density and velocity fluctuations, even the $l = 1$ multipole is affected by power at $k^{-1} > 200$ Mpc only at the 2% level. Due to the small number of large angular modes available on the sky, the expectation value of C_l cannot be measured precisely at small l . Figure 2 shows that this precludes new information from being obtained on scales $k^{-1} \gtrsim 130$ Mpc using angular structure at any given redshift. An optimal observing strategy would be to divide the sky into separate angular pixels of size $\theta \lesssim 2^\circ$, in which the curvature changes distances by only $\theta^2/24 \sim 7 \times 10^{-5}$. This would allow a direct 3D Fourier transform, which is also the most natural way of analyzing radio observations (Morales & Hewitt 2004; Morales 2004).

7. SUMMARY

We have argued that observers should try to measure the anisotropic form of the power spectrum of 21cm fluctuations. Since measurements on large angular scales are not worthwhile, the three-dimensional power spectrum may indeed be measured by dividing the sky into small angular areas. The anisotropy itself, which is due to the effect of peculiar velocities, facilitates a simple separation of the power spectrum into three separate components. One component allows an unambiguous determination of the primordial power spectrum of gas density fluctuations, which if measured will probe basic cosmological parameters as well as inflation. The other two components probe the properties of astrophysical (radiative) sources of 21cm fluctuations.

This work was supported in part by NSF grants AST-0204514, AST-0071019 and NASA grant NAG 5-13292 . R.B. is grateful for the kind hospitality of the Harvard-Smithsonian CfA, and acknowledges the support of an Alon Fellowship at Tel Aviv University and of Israel Science Foundation grant 28/02/01.

REFERENCES

Allison, A. C., & Dalgarno, A. 1969, ApJ, 158, 423
 Barkana, R., & Loeb, A. 2001, Phys. Rep., 349, 125
 Barkana, R., & Loeb, A. 2004, ApJ, submitted.
 Bharadwaj, S., & Ali, S. S. 2004a, MNRAS, 352, 142
 Bharadwaj, S., & Ali, S. S. 2004b, MNRAS, submitted, preprint [astro-ph/0406676]
 Ciardi, B., & Madau, P. 2003, ApJ, 596, 1
 Fan, X., et al. 2002, AJ, 123, 1247
 Field, G. B. 1958, Proc. IRE, 46, 240
 Fisher, K. B., Scharf, C. A., & Lahav, O. 1994, MNRAS, 266, 219
 Furlanetto, S. R., Zaldarriaga, M., & Hernquist, L. 2004a, ApJ, submitted, preprint astro-ph/0403697
 Gnedin, N. Y., & Shaver, P. A. 2003, ApJ, submitted, preprint [astro-ph/0312005]
 Hamilton, A. 1992, ApJ, 385, L5
 Hogan, C. J., & Rees, M. J. 1979, MNRAS, 188, 791
 Kaiser, N. 1987, MNRAS, 227, 1
 Lilje, P. B., & Efstathiou, G. 1989, MNRAS, 236, 851
 Loeb, A., & Zaldarriaga, M. 2004, Phys. Rev. Lett., 92, 211301
 Madau, P., Meiksin, A., & Rees, M. J. 1997, ApJ, 475, 429
 Morales, M. F., ApJ, submitted, preprint astro-ph/0406662
 Morales, M. F., & Hewitt, J., ApJ, in press, preprint astro-ph/0312437
 Santos, M. G., Cooray, A., & Knox, L. 2004, preprint astro-ph/0408515
 Scott, D., & Rees, M. J. 1990, MNRAS, 247, 510
 Sobolev, V. V. 1960, *Moving Envelopes of Stars*, Cambridge: Harvard University Press
 Spergel, D. N., et al. 2003, ApJS, 148, 175
 Tozzi, P., Madau, P., Meiksin, A., & Rees, M. J. 2000, ApJ, 528, 597
 White, R. L., Becker, R. H., Fan, X., & Strauss, M. A. 2003, AJ, 126, 1
 Wouthuysen, S. A., 1952, AJ, 57, 31
 Wyithe, J. S. B., & Loeb, A. 2004, Nature, 427, 815
 Zaldarriaga, M., Furlanetto, S. R., & Hernquist, L. 2004, ApJ, 608, 622
 Zygelman, B. 2004, in preparation